On time scale invariance of random walks in confined space

Daniel Bearup[a,*], Sergei Petrovskii[b]

[a] *ICBM, University of Oldenburg, 26111 Oldenburg, Germany*
[b] *Department of Mathematics, University of Leicester, Leicester, LE1 7RH, UK*

Abstract

Animal movement is often modelled on an individual level using simulated random walks. In such applications it is preferable that the properties of these random walks remain consistent when the choice of time is changed (time scale invariance). While this property is well understood in unbounded space, it has not been studied in detail for random walks in a confined domain. In this work we undertake an investigation of time scale invariance of the drift and diffusion rates of Brownian random walks subject to one of four simple boundary conditions. We find that time scale invariance is lost when the boundary condition is non-conservative, that is when movement (or individuals) is discarded due to boundary encounters. Where possible analytical results are used to describe the limits of the time scaling process. Numerical results are then used to characterise the intermediate behaviour.

Keywords: random walks, time scale invariance, self similarity, confined space

1. Introduction

Movement is always present in wild populations. Even species which are usually individually immobile, such as plants or sessile animals, have some means of dispersal in space, i.e. seed dispersal or a motile life stage. Naturally this movement can have significant effects on population dynamics, particularly if movement mediates interactions, such as predation, between species [1, 2, 3, 4, 5]. Consequently it is beneficial, where possible, to incorporate the effects of movement into mathematical models of populations.

One approach to modelling movement attempts to account for all stimuli that may influence an individual's behaviour [6, 7]. These models can be quite complex and may require detailed information about the individual's environment [8]. As such they are typically used to simulate individual movement tracks rather than population level behaviour. For studies of whole populations

*Corresponding author. Tel: +49-(0)441-7983-612
Email address: daniel.bearup@uni-oldenburg.de (Daniel Bearup)

(consisting of large numbers of individuals) simpler approaches, describing average rather than specific behaviour i.e. mean field models, are usually needed. The diffusion equation is perhaps the most commonly used mean field model [2, 9].

The microscopic theory connecting these approaches is the framework of random walks [10]; for example, the diffusion equation describes the behaviour of the simplest random walk, Brownian motion. By approximating movement by random walks, with known parameters, it is possible to extract the generic effects of movement. For example, a dispersal rate for the population can be derived and used to parameterise diffusion-reaction equations to model spatiotemporal population dynamics [3, 11]. Optimal foraging patterns and encounter rates, with predators or traps, (even in relatively complex environments) have been studied in a similar way [12, 13, 14, 15].

Many random walk models are implemented in discrete time, that is each step takes a finite, non-zero period of time, Δt. It is clearly preferable that the generic properties of the random walk be insensitive to this parameter (scale invariance). Random walks generated by stable distributions have this property in unbounded space [16]. However, despite the ubiquity of boundaries in nature, the effects of time scaling in confined space have not been extensively studied. The only previous study on this subject that we are aware of [17] considers a model system which is not related to animal movement. It demonstrates that random walks with identical characteristics in unbounded space behave measurably differently in a bounded space.

In this paper we undertake a more detailed study of this phenomenon using the drift and diffusion rates of individuals performing a Brownian walk in a bounded space. Section 2 introduces a model framework for individual movement in a bounded space and particularly focuses on how boundaries may be implemented. In a one dimensional system the effects of these boundaries can be described analytically in certain limiting cases. This is discussed in detail in Section 3. Intermediate cases are investigated using numerical simulations. These results are extended to more realistic two dimensional geometries in Section 4. Finally Section 5 summarises these results and discusses their wider relevance.

2. Random walks in a bounded space

The size of individuals, relative to the typical dispersal distances, is usually negligible. Consequently we treat an individual's position as a point, $\mathbf{R}(t) = (x, y)$, and its movement path as a continuous, curvilinear, track in space. However it is relatively rare for individuals to be monitored in anything approaching real time. Instead an individual's location may be recorded on an hourly, or even daily, basis depending on the species traits. Thus the true path is approximated by a series of line segments ($\{\Delta\mathbf{r}_i\}$), Fig. 1, each representing displacement in a fixed time period, Δt [2]. Typically the movement represented by each line segment arises from responses to a multitude of stimuli. Consequently, even if these responses are deterministic, the combined response is likely to be

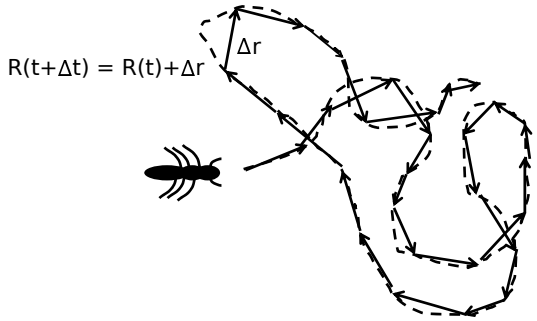

Figure 1: Discretisation of a continuous path using line segments. An individual's position, denoted by $\mathbf{R}(t)$, changes, over a period Δt, by a line segment, $\Delta\mathbf{r}$.

complicated. It is for problems of this type, replacing a complicated deterministic description with a simpler probabilistic one, that statistical mechanics was developed [18]. Thus we simulate movement paths, at a given sampling rate, as random walks by drawing these line segments from a suitably parameterised probability distribution. We will consider Brownian random walks, generated by line segments with normally distributed components, i.e. in two dimensions $\Delta\mathbf{r} = (\Delta x, \Delta y)$ with $\Delta x, \Delta y \sim \mathcal{N}(0, \sigma^2)$.

In this work we are particularly interested in the average movement behaviour of a population of identical individuals performing the same movement pattern. This is typically characterised by two processes: drift, a movement biased in a particular direction, and diffusion, the spread of the population in space, cf [10]. The rates of these processes can be calculated from the mean and mean square displacements of the individuals as follows. The mean displacement is given by:

$$\langle \Delta\mathbf{R}(t) \rangle = \sqrt{\mu_x^2 + \mu_y^2}, \tag{1}$$

where μ_x and μ_y are the mean displacements in the x and y directions respectively. That is:

$$\mu_x = \iint_\Omega (x - x_0) g(x, y) dx dy, \tag{2}$$

where $g(x, y)$ is the position probability density function (pdf) of the population and Ω is the (two dimensional) domain in which the individuals move (μ_y is defined analogously). The mean square displacement is given by:

$$\left\langle \Delta\mathbf{R}^2(t) \right\rangle = \iint_\Omega \left(\sqrt{(x - x_0)^2 + (y - y_0)^2} \right)^2 g(x, y) dx dy. \tag{3}$$

The drift rate, A, and the diffusion coefficient, D, in a two dimensional space are related to these properties as follows [19]:

$$A = \frac{\langle \Delta\mathbf{R}(t) \rangle}{t}, \qquad D = \frac{\left\langle \Delta\mathbf{R}^2(t) \right\rangle - \left\langle \Delta\mathbf{R}^1(t) \right\rangle^2}{4t}. \tag{4}$$

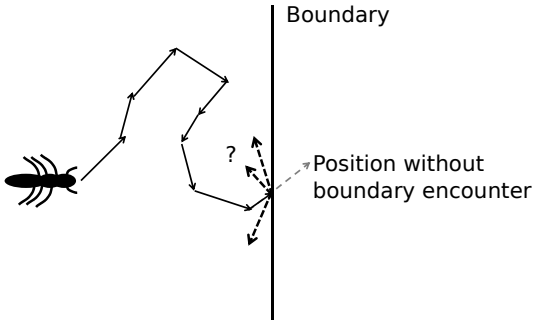

Figure 2: Sketch of the effect of encountering a boundary. A line segment which crosses the boundary is split into two segments, movement prior to the boundary encounter and movement after this event. The bold arrows show possible movement directions after the encounter.

In unbounded space a Brownian random walk has no drift, $A = 0$, and second moment given by $\langle \Delta \mathbf{R}^2(t) \rangle = 2n\sigma^2$, where $n = t/\Delta t$ and σ^2 is the variance of the underlying distribution. Thus the diffusion coefficient is:

$$D = \frac{\sigma^2}{2\Delta t}. \tag{5}$$

This relationship allows us to rescale the random walk while preserving D. For an alternative time scale, $\widetilde{\Delta t} = a\Delta t$, we obtain the same dispersal rate by taking $\widetilde{\sigma}^2 = a\sigma^2$.

However, when an individual encounters a boundary, its movement is modified by that encounter, see Fig. 2. For instance, a barrier which the individual cannot cross, requires that the individual remain within the domain. This interaction clearly reduces the total displacement of that individual and thus its effective speed. Alternatively, encountering a trap will cause the individual to be removed from the population. In this case its movement should no longer contribute to the overall dispersal of the population.

Moreover, the impact of these boundaries may not remain the same under the time-scaling process outlined above. For a relatively coarse time scale, with associated relatively large σ^2, each encounter with a boundary must necessarily introduce a significant change to the behaviour of that individual. For much finer time scales, with concomitantly smaller σ^2 values, the impact of any individual encounter should result in a smaller alteration in individual movement.

The two boundary types above correspond to simple Dirichlet and Neumann boundary conditions (cf. [2, 20]). A boundary which removes an individual from the population can be regarded as an absorbing boundary at which the population goes to zero (a Dirichlet condition). Such a boundary can be implemented in the random walk framework by discarding individuals which encounter it. An impenetrable barrier is represented by a no-flux condition (a Neumann condition). The most common implementation of this boundary condition in the

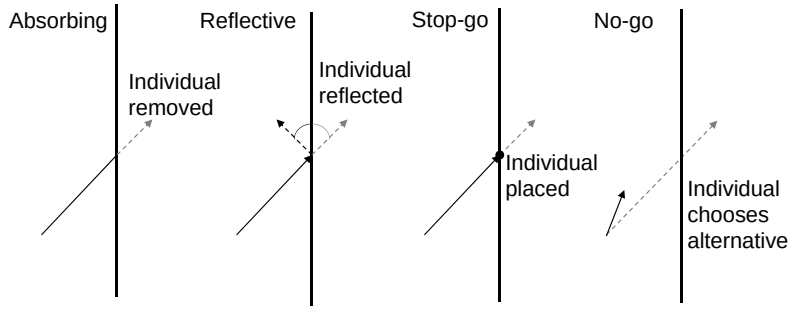

Figure 3: Sketch of different types of boundary effects. Details of these boundary types can be found in the text.

random walk framework treats the individual's movement after the encounter as if it were perfectly reflected in the boundary, see, for example, [2]. A natural extension of this model considers an inelastic reflection, where the individual loses energy in the encounter and thus does not rebound so far as in the first case. In its most extreme form this results in the individual simply stopping at the boundary where the encounter took place. These models treat cases where the individual has no knowledge of the boundary. An alternative is to model the case where the individuals know the location of the boundary and choose not to cross it [21]. This is achieved by selecting steps that remain within the domain. These different types of boundary encounter are sketched in Figure 3.

3. Behaviour of populations on a bounded line

In the previous section we discussed how the proximity of a population to a boundary may affect its rate of dispersal. In this section we aim to make these intuitive ideas more quantitative. While real populations are typically able to move in at least two dimensions, we initially restrict our attention to populations constrained to move in a single dimension. In particular, individuals are assumed to exist on a half line, $0 \leq x < \infty$, with either an impenetrable or an absorbing boundary at $x = 0$.

We consider random walks of duration t (without loss of generality $t = 1$) consisting of a finite number of steps of constant duration, $\Delta t \in (0, 1]$. It is then clear that there are two limiting cases of the time-scaling process; referred to as the **one step limit** and the **infinite step limit**. The **one step limit** corresponds to taking $\Delta t = t = 1$, and is the coarsest possible random walk as it contains a single step. Naturally the **infinite step limit**, obtained as $\Delta t \to 0$, is a smooth random walk which contains an infinite number of steps. It is relatively straightforward to derive the mean and variance of Brownian random walks analytically for these limiting cases.

In particular, the final position, x_1, of an individual, released at x_0, is characterised by a probability density function (pdf). For a single step random walk

one step limit	pdf ($x \geq 0$)	
(i) reflective	$f'_r = f(x_1; x_0, \sigma^2) + f(-x_1; x_0, \sigma^2)$	[2]
(ii) stop-go	$f'_s = \begin{cases} \frac{1}{2}\left(1 - \text{erf}\left(\frac{x_0}{\sqrt{2\sigma^2}}\right)\right)\delta(x) & x_1 = 0 \\ f(x_1; x_0, \sigma^2) & x_1 > 0 \end{cases}$	
(iii) no-go	$f'_n = 2f(x_1; x_0, \sigma^2) / \left(1 + \text{erf}\left(\frac{x_0}{\sqrt{2\sigma^2}}\right)\right)$	[21]
(iv) absorbing	$f'_a = 2f(x_1; x_0, \sigma^2) / \left(1 + \text{erf}\left(\frac{x_0}{\sqrt{2\sigma^2}}\right)\right)$	
infinite step limit	**pdf ($x \geq 0$)**	
(v) impenetrable	$f_i^{(\infty)} = f(x_1; x_0, 2Dt) + f(-x_1; x_0, 2Dt)$	[20, 22]
(vi) absorbing	$f_a^{(\infty)} = (f(x_1; x_0, 2Dt) - f(-x_1; x_0, 2Dt)) / \text{erf}\left(\frac{x_0}{\sqrt{4Dt}}\right)$	[20, 22]

Table 1: Probability density functions for Brownian random walks on the half line. Note that f refers to Eq. (6).

this pdf can be obtained by applying the chosen boundary condition to the step length distribution used. For random walks with multiple steps deriving the pdf of the final position in this way becomes increasingly difficult as more steps are added, i.e. as Δt decreases, see Appendix A. However, in the infinite step limit we satisfy the conditions used when deriving the mean field approximation of this system, i.e. the diffusion equation. A pdf for the position of a walker, $u(x,t)$, can then be obtained by solving this equation subject to appropriate initial and boundary conditions. Having obtained such a pdf the mean and variance for any given release point, x_0, can be found as discussed in Section 2.

These limiting cases provide a structure for the time-scaling process. However to completely understand its effects on random walks we must also consider intermediate choices of Δt. Since the position pdfs in these cases can be quite complex they are analysed with numerical simulations rather than analytically. We begin by considering the effects of an impenetrable boundary.

3.1. Effects of an impenetrable boundary

As noted in Section 2 there are several ways to implement an impenetrable boundary: individuals may bounce off the boundary (a **reflective boundary**); they may stop temporarily at the boundary (a **stop-go boundary**); or they may only choose steps that remain within the domain (a **no-go boundary**). In the infinite step limit, as $\Delta t \to 0$, we would expect any differences between these cases to disappear allowing a simple no-flux Neumann condition, $\frac{\partial u}{\partial x}\big|_{x=0} = 0$ for $t > 0$, to be used.

For the one step limit we must find the pdf describing the position of an individual after a single step. As noted above, in unbounded space this is simply $x_1 \sim \mathcal{N}(x_0, \sigma^2)$. In particular, the probability that a position x_1 is

attained given a start position of x_0 is given by [2]:

$$\mathbb{P}(x_1 \mid x_0) = f(x_1; x_0, \sigma^2) = \frac{1}{\sqrt{2\pi\sigma^2}} \exp\left(-\frac{(x_1 - x_0)^2}{2\sigma^2}\right). \tag{6}$$

In the bounded domain, the tail, $x_1 < 0$, cannot occur; the boundary condition used determines how steps from this tail are returned to the domain. The reflective boundary is the most straightforward, the negative tail is simply folded back into the domain. For the stop-go boundary such steps are treated as if they end at the boundary. Thus the probability density at the boundary is set equal to probability density in the tail. Finally, for the no-go boundary, we select steps that remain within the boundary. This amounts to discarding steps in the negative tail and rescaling the pdf so that its total density is 1. This is achieved by dividing by the probability density remaining within the domain. The pdfs describing the effects of these boundary conditions, analogous to Eq. (6), can be found in Table 1 (rows (i)-(iii)).

For the infinite step limit, the pdf is a solution of the diffusion equation:

$$\frac{\partial u}{\partial t} = D\frac{\partial^2 u}{\partial x^2}, \tag{7}$$

for a point source initial condition and as such a Green's function. The (well-known) solution for a no-flux boundary condition is given in Table 1 (row (v)) in terms of Eq. (6) to aid comparison. Recalling Eq. (5), and that $\Delta t = 1$ in the one step limit, we have $D = \sigma^2/2$. Substituting this expression for D and $t = 1$ into this pdf yields the pdf for the one step limit with a reflective boundary, Table 1 (rows (i)). Thus the behaviour of these two cases is identical.

The mean and variance of these distributions can be obtained straightforwardly by standard techniques so we omit the details of their derivation. The resulting functions are given in Table 2 and they are plotted against the release point, x_0, in Fig. 4A-B. We observe first that, in all cases, individuals released close to the boundary exhibit a non-zero drift (i.e. mean) away from it. As the release point is moved away from the boundary this drift decays monotonically and becomes indistinguishable from zero (the drift for a Brownian walk in unbounded space) for $x_0 > 3.5$. Similarly, individuals released close to the boundary have a relatively small diffusion rate (i.e. variance) which increases monotonically to become indistinguishable from one, again the value that is obtained in unbounded space, at the same distance from the boundary.

We have already noted that the behaviour of these random walks in the infinite step limit does not depend on how the boundary is implemented. Furthermore for the reflective boundary the behaviour in the one step limit is identical to that in the infinite step limit (Curve 1 in Fig. 4). This suggests that, in this case, temporal rescaling of the random walk has no impact on the movement characteristics of individuals. In contrast, the behaviour in one step limit for the stop-go and no-go boundaries (Curves 2 and 3 respectively) differs from that obtained in the infinite step limit. In particular, the stop-go boundary induces about half as much drift in the one step limit compared to the infinite step limit

property	cases	function ($x_0 \geq 0$)	
mean	(i), (v)	$\sqrt{\frac{2\sigma^2}{\pi}}\exp\left(\frac{-x_0^2}{2\sigma^2}\right) - x_0\left(1-\mathrm{erf}\left(\frac{x_0}{\sqrt{2\sigma^2}}\right)\right)$	[23]
	(ii)	$\sqrt{\frac{\sigma^2}{2\pi}}\exp\left(\frac{-x_0^2}{2\sigma^2}\right) - \frac{x_0}{2}\left(1-\mathrm{erf}\left(\frac{x_0}{\sqrt{2\sigma^2}}\right)\right)$	
	(iii), (iv)	$\sqrt{\frac{2\sigma^2}{\pi}}\exp\left(\frac{-x_0^2}{2\sigma^2}\right) / \left(1+\mathrm{erf}\left(\frac{x_0}{\sqrt{2\sigma^2}}\right)\right)$	
	(vi)	$x_0\left(1/\,\mathrm{erf}\left(\frac{x_0}{\sqrt{2\sigma^2}}\right) - 1\right)$	
variance	(i), (v)	$\sigma^2\left(1-\frac{2}{\pi}\exp\left(\frac{-x_0}{\sigma^2}\right)\right) - \sqrt{\frac{8\sigma^2x_0^2}{\pi}}\exp\left(\frac{-x_0^2}{2\sigma^2}\right)\mathrm{erf}\left(\frac{x_0}{\sqrt{2\sigma^2}}\right) + x_0^2\left(1-\mathrm{erf}^2\left(\frac{x_0}{\sqrt{2\sigma^2}}\right)\right)$	[23]
	(ii)	$\frac{\sigma^2}{2}\left(1+\mathrm{erf}\left(\frac{x_0}{\sqrt{2\sigma^2}}\right) - \frac{1}{\pi}\exp\left(\frac{-x_0}{\sigma^2}\right)\right) - \sqrt{\frac{\sigma^2x_0^2}{2\pi}}\exp\left(\frac{-x_0^2}{2\sigma^2}\right)\mathrm{erf}\left(\frac{x_0}{\sqrt{2\sigma^2}}\right) + \frac{x_0^2}{4}\left(1-\mathrm{erf}^2\left(\frac{x_0}{\sqrt{2\sigma^2}}\right)\right)$	
	(iii), (iv)	$\sigma^2\left(1-\frac{2}{\pi}\exp\left(\frac{-x_0^2}{\sigma^2}\right) / \left(1+\mathrm{erf}\left(\frac{x_0}{\sqrt{2\sigma^2}}\right)\right)^2\right) - \sqrt{\frac{2\sigma^2x_0^2}{\pi}}\exp\left(\frac{-x_0^2}{2\sigma^2}\right) / \left(1+\mathrm{erf}\left(\frac{x_0}{\sqrt{2\sigma^2}}\right)\right)$	
	(vi)	$\sigma^2 + x_0^2\left(1-1/\,\mathrm{erf}^2\left(\frac{x_0}{\sqrt{2\sigma^2}}\right)\right) + \sqrt{\frac{2\sigma^2x_0^2}{\pi}}\exp\left(\frac{-x_0^2}{2\sigma^2}\right) / \,\mathrm{erf}\left(\frac{x_0}{\sqrt{2\sigma^2}}\right)$	

Table 2: Mean and variance of pdfs (denoted by Roman numerals) in Table 1. The functions for the infinite step limit (cases (v) and (vi)) can be converted to their diffusion forms by taking $\sigma^2 = 2Dt$.

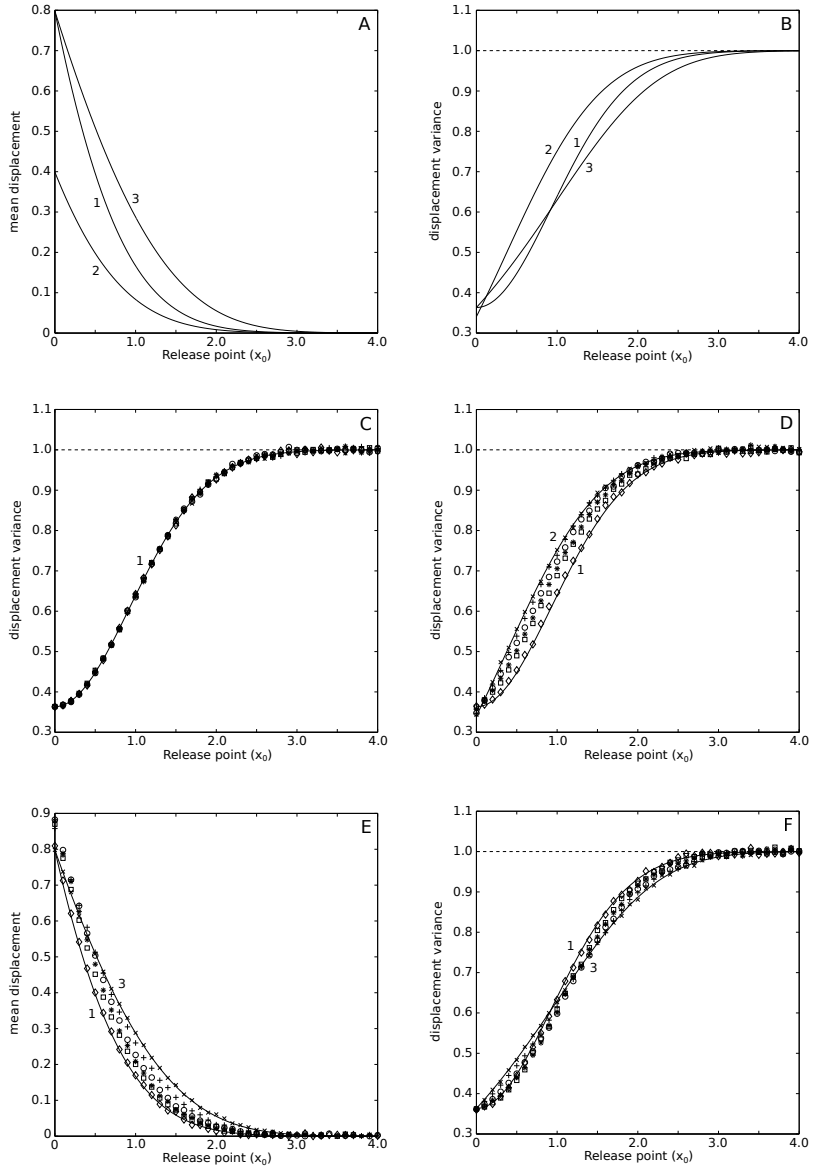

Figure 4: Plots of mean (A, E) and variance (B, C, D, F) profiles for individuals subject to an impenetrable boundary. Solid curves labelled 1 correspond to the infinite step limit and the one step limit for the reflective boundary. Solid curves labelled 2 or 3 correspond to the one step limit for stop-go or no-go boundary conditions respectively. The dashed reference line shows the variance that would be obtained in unbounded space. The remaining curves (symbols) were obtained numerically using the following Δt values: 1 - $\times$, 0.5 - $+$, 0.25 - $\circ$, 0.125 - $*$, 0.0625 - $\square$, 0.001 - $\diamond$, for a reflective (C), stop-go (D) or no-go (E-F) boundary.

and has a convex rather than sigmoidal diffusion profile. The no-go boundary induces more drift in this limit than in the infinite step limit and has a lower curvature diffusion profile. Thus it is natural to investigate how these profiles change for intermediate values of Δt.

The analytical approach used to obtain these profiles for the one step limit can be extended to deal with intermediate values of Δt, see Appendix A. However this analysis becomes increasingly complex as more steps are added to the random walk, so we use a numerical approach here. An individual was initially placed at a point, x_0, on the half line, H. The positions taken by this individual, over a time period of one time unit, were then generated using random numbers drawn from a normal distribution, $\mathcal{N}_{\Delta t} = \mathcal{N}(0, 1/\Delta t)$. (Note that this choice of distribution ensures that all random walks have the same effective speed, D.) If an individual crossed the boundary, reaching a position $-x$, the appropriate boundary condition was applied. In particular for a reflective boundary it was placed at x, for a stop-go boundary it was placed at the boundary, and for a no-go boundary an alternative step was generated (accepting only steps that produced a final position within the domain). The mean and variance of the displacement, from x_0, of individuals was computed on completion of their random walk. The mean squared displacement at a point was estimated from repeated (a total of 100000) simulations of individuals (with steps drawn from the same normal distribution) released at that point. Six time scales were used, $\Delta t \in \{1, 0.5, 0.25, 0.125, 0.0625, 0.001\}$. Resulting profiles for an array of release points 0.1 units apart are plotted in Fig. 4C-F.

As we expected the drift (not shown) and diffusion (Fig. 4C) for the reflective boundary are independent of Δt. For all choices of Δt considered the values calculated lie on, or close to, the solutions obtained from the limiting cases. (In fact this can be readily proven analytically, see Appendix Appendix A.) Variations from these solutions can reasonably be ascribed to the stochastic method used to obtain these intermediate values. For the stop-go and no-go boundaries we obtain similarly good agreement between the simulated profiles for $\Delta t = 1$ and $\Delta t = 0.001$ and the corresponding limiting cases, Fig. 4D-F. For the stop-go boundary the intermediate curves appear to shift monotonically between the two limiting cases of the diffusion profile, we see in Fig. 4D that the symbols all tend to appear in the same order (except where the limiting cases are very close together). A similar pattern (not shown) was observed for the drift profiles and for the no-go boundary for release points far from the boundary, Fig. 4E-F. However for release points close to a no-go boundary the pattern changes. This is most clearly seen from the drift profiles, Fig. 4E. Here, for $x_0 < 0.5$, decreasing Δt initially increases the drift relative to that obtained in the one step limit. As Δt decreases further the drift peaks (for any given release point) and then decreases towards the value obtained in the infinite step limit. For the diffusion profiles, Fig. 4F, this pattern appears to persist further from the boundary, up to $x_0 = 1.2$, but it is less clear since the limiting cases are relatively close together.

We now undertake a similar analysis replacing the impenetrable boundary used here with an absorbing boundary.

3.2. Effects of an absorbing boundary

Individuals which encounter an absorbing boundary are removed from the domain. In the infinite step limit this is modelled by a Dirichlet condition, $u(0,t) = 0$ for $t > 0$.

As in the previous section, we determine the position pdf for the one step limit by modifying Eq. (6) to take into account how positions $x < 0$ are treated by the absorbing boundary condition. Individuals encountering this boundary are removed from the population, terminating the random walk, effectively discarding these positions. Note that this means that the probability of remaining within the domain is less than one. However, since we only compute the displacement of individuals remaining in the domain, we effectively rescale the probability densities of positions within the domain by the probability of remaining within the domain. Thus the pdf obtained, Table 1 (row iv), is equivalent to that obtained for the no-go boundary condition although the mechanism by which it is obtained is subtly different. Note that for $\Delta t < 1$ the pdfs obtained in these two cases are different, Appendix A. Similarly, for infinite step limit the pdf is a Green's function for Eq. (7) and is again well-known, Table 1 (row vi).

The mean and variance of these pdfs are given in Table 2 and plotted in Fig. 5A-B. The drift and diffusion profiles for the absorbing boundary exhibit similar characteristics to those obtained for the impenetrable boundary. In particular the drift profiles are monotone decreasing, the diffusion profiles are monotone increasing, and all profiles become indistinguishable from the values obtained in unbounded space for $x_0 > 3.5$. As for the stop-go and no-go boundary conditions the limiting cases behave differently. For example, close to the boundary the drift and diffusion are larger in the infinite step limit (Curve 2) than in the one step limit (Curve 1).

As for the impenetrable boundary the limiting cases provide only a partial characterisation of the effect of the choice of time scale. Thus we investigate intermediate values of Δt using numerical simulations. The technical details of these simulations are as described in Section 3.1, with the exception of treatment of the boundary. As noted above individuals that encounter an absorbing boundary are removed from the population. This is implemented by terminating random walks that cross the boundary and not including them in calculations of displacement. Note that this means the profiles are typically computed from less than the full 100000 individuals released at each point. The resulting variance profiles are plotted in Fig. 5C.

Once again we find that simulated results for the extreme values of Δt (1.0 and 0.001) are close to the respective limiting cases. Furthermore, the intermediate mean (not shown) and variance profiles appear to move monotonically between the limiting cases in much the same way as they do for the stop-go boundary.

This characterisation of mean and variance profiles confirms that the presence of boundaries does indeed change the way random walks scale with their time step. In the following section we discuss the mechanisms causing this behaviour.

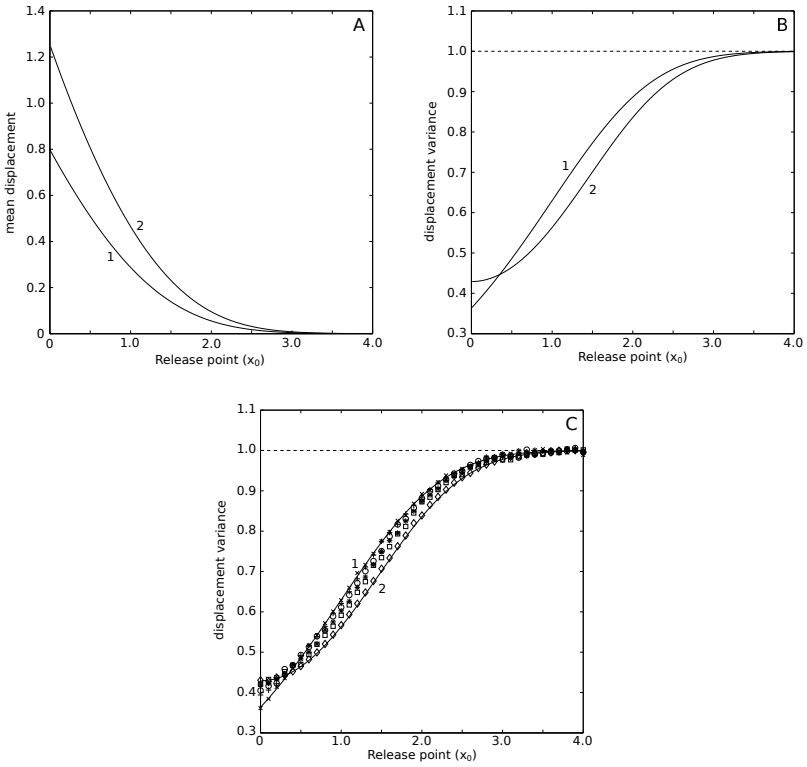

Figure 5: Plots of mean (A) and variance (B, C) profiles for individuals subject to an absorbing boundary. Solid curves labelled 1 or 2 correspond to the one step or infinite step limits respectively. The dashed reference line shows the variance that would be obtained in unbounded space. The remaining curves (symbols) were obtained numerically using the following Δt values: 1 - $\times$, 0.5 - $+$, 0.25 - $\circ$, 0.125 - $*$, 0.0625 - $\square$, 0.001 - $\diamond$.

3.3. Interpretation and discussion of results

Our results so far are as follows:

1. Proximity to a boundary induces a drift away from that boundary and reduces the diffusion rate relative to that which would be obtained in unbounded space.
2. Nonetheless time scale invariance of the drift and diffusion rates can be preserved for the reflective implementation of the impenetrable boundary.
3. For the stop-go, no-go and absorbing boundary conditions time scale invariance of these properties is lost, at least if Eq. (5) is used.

We observed in Section 2 that any given encounter with an impenetrable boundary would reduce the displacement of the individual involved. However, with respect to the average movement characteristics of the individual, this has an effect which may appear unintuitive. In particular, while individuals near such a boundary diffuse relatively slowly they also appear, on average, to move away from the boundary in a directed manner. This can be explained by considering the relative amount of space to either side of the individual's release point, cf [24]. Individuals released close to the boundary are more likely to end their random walk further from the boundary than where they started than vice versa because the amount of space, x_0, between their release point and the boundary (**the confined side**) is relatively small. This accounts for the observed drift away from the boundary. Similarly, because these individuals tend to move in one direction, the amount they spread out, another interpretation of the diffusion rate, is reduced. As the space on the confined side increases the probability that an individual will end its movement in this region increases and thus the drift and diffusion rates become closer to what would be found in an unbounded space.

For the reflective implementation of this boundary the choice of Δt has no effect. This is not the case for the stop-go and no-go boundary conditions where the drift and diffusion rates depend on this value. These differences can be explained by in terms of the confinement effects described above. Consider first one step random walks ($\Delta t = 1$) for release points close to reflective or stop-go boundaries. In order for an individual's final position to be on the confined side for the reflective boundary it must make a step towards the boundary of length less than two times x_0. A longer step results in the individual being reflected past its start point. In contrast, since an individual stops when it encounters a stop-go boundary, any step towards the boundary leaves the individual on the confined side for this boundary. Thus for this Δt individuals are more likely to end their movement on the confined side for the stop-go boundary than for the reflective boundary; thus the drift for the stop-go boundary is lower. The diffusion rate is also reduced for such release points since a large number of individuals $\approx 50\%$ end their movement in the same place, i.e. on the boundary, further reducing the spread that can be attained. However as x_0 increases, the diffusion rate increases faster for the stop-go boundary than for the reflective boundary. This is because for the reflective boundary individuals are more likely

to be distributed throughout the confined side, while for the stop-go boundary many individuals end their movement at the extreme edge of this space (i.e. the boundary). This tends to exaggerate the spread for the stop-go boundary relative to the reflective boundary.

The effects of the no-go boundary can be analysed in the same way. In particular, for this boundary an individual's final position will be on the confined side only if it makes a step towards the boundary of length less than x_0, since longer steps are discarded. Except for release points on the boundary, the probability of this is lower than for the reflective boundary, where steps of length less than $2x_0$ achieve the same effect. Thus the drift for the no-go boundary is higher (except at the boundary) than for the reflective boundary. This reduced probability of ending movement on the confined side also impacts the diffusion rate. When the confined side is small the spread that can be attained in this region is relatively small. Thus a higher spread is observed for the no-go boundary, relative to the reflective boundary, since fewer individuals end their movement in this area. However, this spread is biased towards the unconfined side. As the release point is moved away from the boundary the confined side becomes bigger, allowing a higher spread to be achieved by distributing evenly on both sides of the boundary. This results in the no-go boundary producing a lower diffusion rate for intermediate release points than the reflective boundary.

As Δt decreases the number of steps in the random walk increases and the length of individual steps decreases. Thus the truncation of a given step by an encounter with a stop-go boundary is smaller or, in other words, the inelasticity of this boundary is reduced. Similarly it becomes less likely that a given step would encounter a no-go boundary and thus be discarded in favour of a step which did not encounter the boundary. Thus as Δt decreases the mechanistic differences in effect of the stop-go and no-go boundaries relative to the reflective boundary decrease and so the drift and diffusion rates for these boundaries become more similar.

A loss of time scale invariance is also observed for the absorbing boundary condition. In this case, however, this is not just an effect of the relative sizes of the confined and unconfined sides of the domain, but also the probability of encountering the boundary during a given random walk, see Fig. 3.3. In the one step and infinite step limits these probabilities are given by $(1-\text{erf}(x_0/\sqrt{2\sigma^2}))/2$ and $1-\text{erf}(x_0/\sqrt{4Dt})$ respectively. For a one step random walk an individual has a single chance to encounter the boundary, equal to the probability that the step taken is towards the boundary and is greater that x_0. Since individuals that encounter this boundary do not contribute to the drift and diffusion rates, this results in the same relative probabilities of ending movement on the confined and unconfined sides of the domain as for the no-go boundary. Thus, for a one step random walk, the drift and diffusion profiles are the same for these two boundary types.

However as Δt decreases the number of steps, and hence the number of opportunities for an individual to encounter the boundary, increases. This causes the probability of such an encounter to increase, this can be seen quite clearly in Fig. 3.3B . Note though, that this probability is still related to the individual's

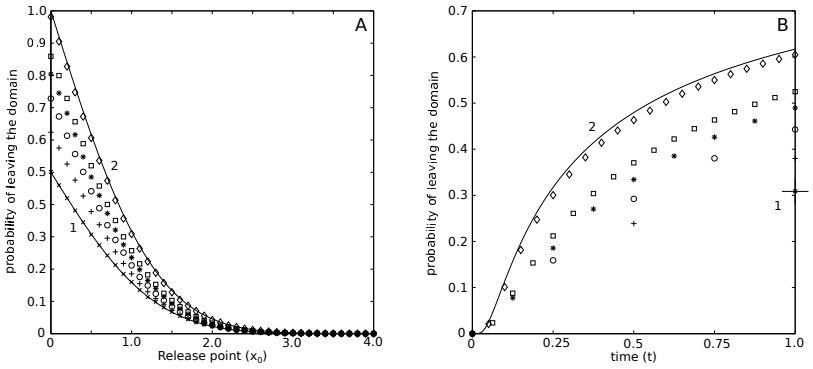

Figure 6: Plots of the probability of leaving the domain against position of release (A) and time (B). Solid curves correspond to the one step (1) and infinite step (2) limits. The remaining curves (symbols) were obtained numerically using the following Δt values: 1 - $\times$, 0.5 - $+$, 0.25 - $\circ$, 0.125 - $*$, 0.0625 - $\square$, 0.001 - $\diamond$. A single release point, $x_0 = 0.5$, was used for B.

proximity to the boundary, an individual close to the boundary is more likely to encounter it that an individual far from it. These factors combine to cause the probability of an individual not encountering the boundary but remaining close to it to decrease as Δt decreases thus causing the drift to increase. For release points close to the boundary this also results in an increased spread and hence diffusion rate, as many walks which would have relatively low spread are eliminated by boundary encounters. However, as x_0 increases the displacement of random walks that encounter the boundary increase. The loss of these walks with relatively high spread causes the diffusion rate to grow relatively slows as x_0 increases.

Loss of time scale invariance appears to be associated with boundary conditions which require that some component of the random walk be discarded. The stop-go, no-go, and absorbing boundary conditions discard movement distance, movement steps or individuals respectively when the boundary would be crossed. In contrast, the reflective boundary condition preserves both movement (by transferring it back into the domain) and individuals and displays time scale invariance.

While this one dimensional analysis provides an interesting insight into the behaviour of individuals near a boundary, in nature individuals are rarely constrained to a single dimension. In the following section we show that these results generalise to a two dimensional domain.

4. Behaviour of populations in two dimensional geometries

We have found that, in proximity to a boundary, the movement characteristics of a population of random walkers varies from that obtained in unbounded

space. Furthermore it appears that loss of time scale invariance is associated with boundary conditions which are non-conservative, see Section 3.3. However our work to this point has been restricted to a simple, but unrealistic, one dimensional space. In practice individuals will usually be able to move in an, at least, two dimensional space. The numerical approach used in Sections 3.1 and 3.2 can be readily generalised to handle this problem.

Note that in this two dimensional setting, the shape of the boundary, in addition to the type of boundary condition applied, may have an effect on behaviour. We consider three basic cases: (1) a half plane $H = [0, \infty) \times \mathbb{R}$, analogous to the half line used in Section 3; (2) a finite domain $F = [-L, L] \times [-L, L]$, corresponding to a habitat which individuals cannot leave; and (3) an infinite domain with an internal boundary $I = \mathbb{R}^2/[-l, l] \times [-l, l]$, corresponding to an effectively unlimited habitat which contains a region which individuals cannot enter. The second two domains contain different types of corners, concave or convex, which we can reasonably expect to impact individual movement differently.

4.1. Decomposition into a sum of one dimensional measures

The drift and diffusion rates in a two dimensional geometry can be calculated by the same methods as were used in Section 3. In general, however, deriving analytical solutions to integrals in two dimensions is much more difficult than in one dimension, except for certain special cases. One special case, that of a multiplicatively separable function $u(x, y) = X(x)Y(y)$, in a rectangular domain, is useful for the first two geometries that we consider. The integral of such a function, in such a domain can be written as a product of the integrals of the individual functions:

$$\iint_{\Omega} u(x, y)dydx = \int_{\Omega_x} X(x)dx \cdot \int_{\Omega_y} Y(y)dy, \tag{8}$$

since these individual functions are constant with respect to the other variable, see for example [25].

If the x and y components of a two dimensional random walk are independent then $\mathbb{P}((x_1, y_1)|(x_0, y_0)) = \mathbb{P}(x_1|x_0)\mathbb{P}(y_1|y_0)$. Thus the pdf of this random walk can be written as the product of the pdfs of the x and y components, $g(x, y) = g_x(x)g_y(y)$, and so it multiplicatively separable. (Note that when the diffusion equation can be solved by separation of variables the resulting pdf is automatically separable.) Thus the mean square displacement, Eq. (3), of such a random walk becomes:

$$\left\langle \Delta\mathbf{R}^2(t) \right\rangle = \int_{\Omega_x} (x-x_0)^2 g_x(x)dx \cdot \int_{\Omega_y} g_y(y)dy + \int_{\Omega_x} g_x(x)dx \cdot \int_{\Omega_y} (y-y_0)^2 g_y(y)dy. \tag{9}$$

By definition the integral of a pdf over the entirety of its domain is one so this expression reduces to the sum of the mean square displacements in the x and y directions:

$$\left\langle \Delta\mathbf{R}^2(t) \right\rangle = \int_{\Omega_x} (x - x_0)^2 g_x(x)dx + \int_{\Omega_y} (y - y_0)^2 g_y(y)dy. \tag{10}$$

Furthermore, for a random walk with independent components, the drifts, μ_x and μ_y, are exactly the drifts in the x and y directions, i.e.:

$$\mu_x = \iint_\Omega (x - x_0) g(x, y) dx dy = \int_{\Omega_x} (x - x_0) g_x dx \cdot 1. \tag{11}$$

Thus the mean and variance of such a random walk are exactly the sum of the mean and variance of its components [26].

4.2. Individuals on a half plane

The half plane closely resembles the half line, in that an individual's proximity to the boundary is determined entirely by its position in the x dimension. However the additional freedom of movement, allowed by the y dimension, does affect the drift and diffusion rates. We consider random walks with x and y components distributed normally with variance 1.0. Variance profiles from simulated random walks, with $\Delta t \in \{1, 0.5, 0.25, 0.125, 0.0625, 0.001\}$ as in Section 3, are plotted for each of the boundary conditions in Fig. 7A-D.

For the reflective, no-go, and absorbing boundary conditions the x and y components of the random walk are independent; that is, for individuals that remain in the domain, the length of steps in the x or y direction have no effect on the lengths of steps in the other direction. In particular their pdfs can be written as $f'_{2d,\text{type}}(x, y) = f'_{\text{type}}(x) f(y)$, where type is r, n, or a for the reflective, no-go, or absorbing boundary conditions respectively. Consequently, as discussed in Section 4.1, the mean and variance for random walks subject to these boundary conditions can be obtained by summation of the mean and variance of the respective components. Since the y component of the random walk is unbounded it contributes drift and diffusion rates of zero and one respectively. The mean and variance of the x component of the random walk is the same as would be obtained in a one dimensional space. The numerical results are in good agreement with variance profiles generated from this decomposition, see Fig. 7A,C-D.

Individuals encountering a stop-go boundary stop at the point where the encounter occurs. The y component of such individuals' position is determined by the angle of the step Δr which causes the encounter. Since this angle is dependent on both x and y the components of the random walk are not independent in this case. Consequently the variance profile generated by the decomposition above produces a significant over-estimate of the diffusion rate attained by individuals subject to this boundary condition, see Fig. 7B. A modification to the stop-go boundary, stopping the individual's movement in the x direction but not in the y direction when the encounter occurs, restores the independence of the two components. For this modification the numerical results correspond well to the limiting case obtained via this decomposition, see Fig. 8.

As noted previously in the infinite step limit we can obtain the pdfs by solving the diffusion equation. For this geometry, and the Neumann and Dirichlet conditions used in Section 3, these solutions are known [20] and are separable. (Note that the solution for the Neumann boundary is identical to the pdf for the

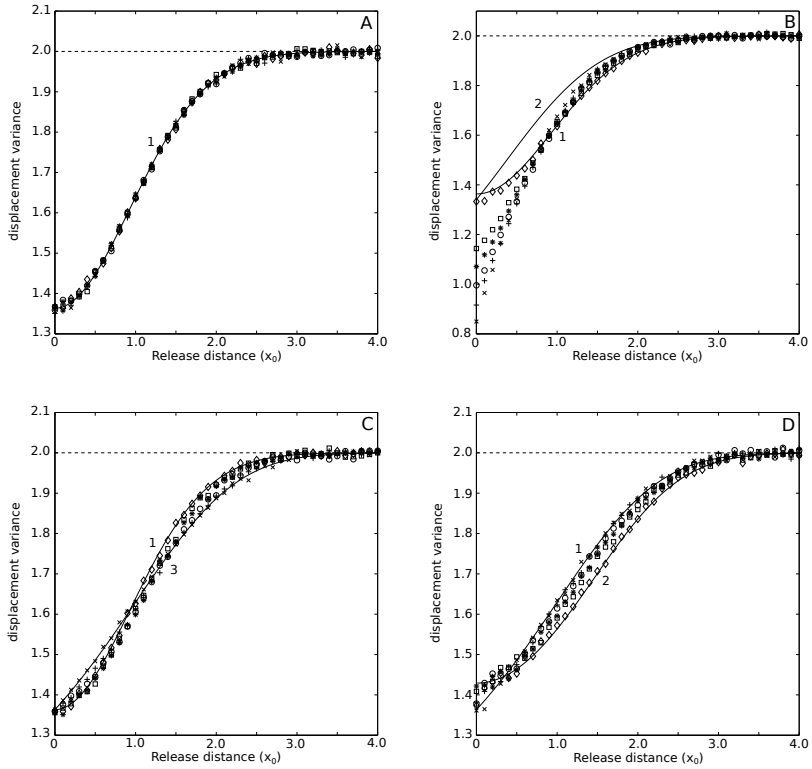

Figure 7: Variance profiles for individuals in the half plane for an impenetrable (A-C) or absorbing (D) boundary. Solid curves were obtained analytically from decomposition into the 1d limiting cases; numbering is consistent with Fig. 4 for A-C and Fig. 5 for D. The dashed reference line shows the variance that would be obtained in unbounded space. The remaining curves (symbols) were obtained numerically using the following Δt values: 1 - $\times$, 0.5 - $+$, 0.25 - $\circ$, 0.125 - $*$, 0.0625 - $\square$, 0.001 - $\diamond$, for a reflective (A), stop-go (B), no-go (C), or absorbing (D) boundary.

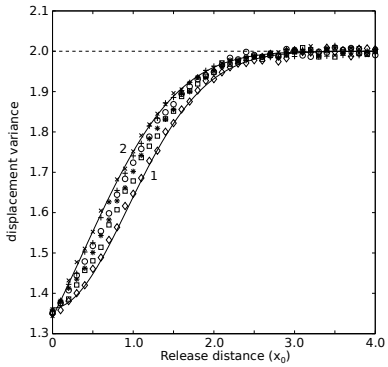

Figure 8: Variance profiles for individuals in the half plane for a modified stop-go boundary (details in the text). Solid curves were obtained analytically from decomposition into the 1d limiting cases; numbering is consistent with Fig. 4. The dashed reference line shows the variance that would be obtained in unbounded space. The remaining curves (symbols) were obtained numerically using the following Δt values: 1 - $\times$, 0.5 - $+$, 0.25 - $\circ$, 0.125 - $*$, 0.0625 - $\square$, 0.001 - $\diamond$.

reflective boundary.) Thus the mean and variance profiles can be obtained by decomposition into one dimensional components as above. Once again the numerical results for $\Delta t = 0.001$ are in good agreement with the variance profiles obtained via this decomposition, see Figs. 7A-D and 8.

Finally we observe that the transition between the limiting cases of the time scaling process is unaffected by the shift to a two dimensional geometry. That is, for the stop-go and absorbing boundaries the transition is monotonic, while for the no-go boundary it is not.

We can reasonably expect that the time scaling behaviour described here will be preserved in some regions of a domain with sufficiently long straight boundaries. We have observed so far that drift and diffusion rates become indistinguishable from those obtained in unbounded space for release points sufficiently far from a single boundary. In the same way we would expect that individuals released close to one boundary but sufficiently far from any other boundaries would behave approximately as described here. However for release points near the corners of a domain, or between two parallel boundaries that are close together, we must account for the effects of both boundaries. In the following section we consider the square domain, F, described above.

4.3. Individuals in a square finite domain

The independence (or otherwise) of the x and y components of random walks is unaffected by the change from the half plane to the finite domain, $F_5 = [-5, 5] \times [-5, 5]$. Thus it is possible to express both of the infinite step limits and the one step limits for the reflective, no-go, and absorbing boundaries as decompositions into one dimensional cases. However, rather than derive the

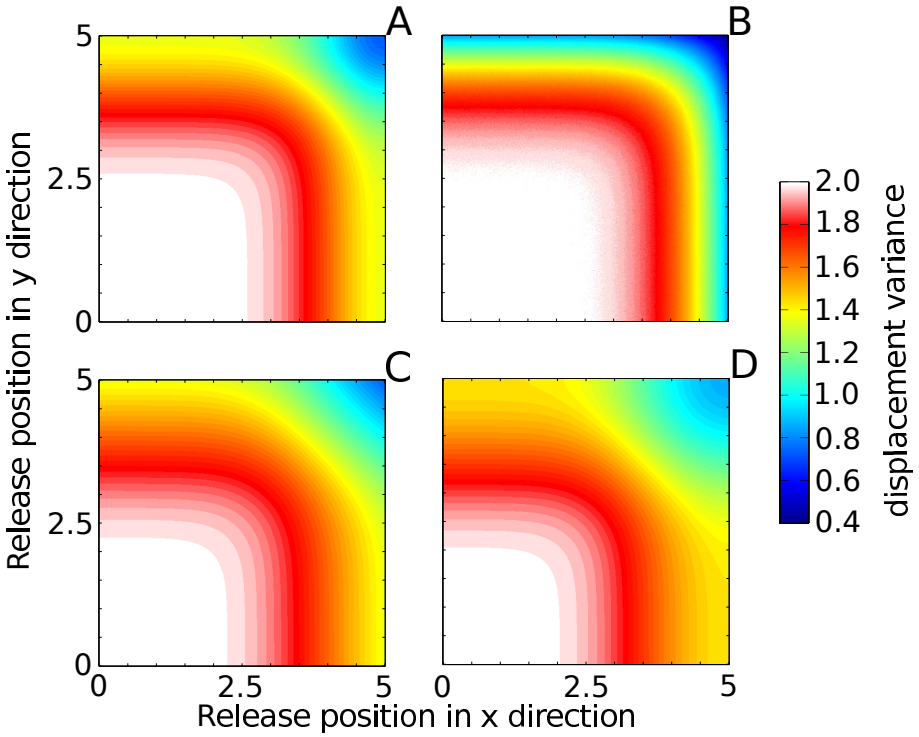

Figure 9: Approximate limiting cases of the variance profiles for individuals released in the upper right quadrant of the finite domain, F. One step limits are plotted in A, B, and C for the reflective, stop-go, and no-go/absorbing boundaries respectively. A is also the infinite step limit for the impenetrable boundary, while its counter part for the absorbing boundary is plotted in D. Note that the one step limit for the stop-go boundary was obtained numerically. (Color online.)

appropriate one dimensional results for a finite domain, we instead approximate these limiting cases from the results obtained for a semi-finite domain in Section 3[1]. Given that the mean and variance for release points further than 3.5 units from any of these boundaries are indistinguishable from those obtained in unbounded space this is a reasonable approximation. Furthermore the resulting approximate limiting cases of the variance, Fig. 9A,C-D, were found to be in good agreement with numerical results. A variance profile for the stop-go boundary in the one step limit was calculated numerically, see Fig. 9B.

The variance profiles for the limiting cases, Fig. 9, display certain common

[1]Pdfs for the one step limit can be obtained by an extension of the method presented in Section 3. The appropriate pdfs for the infinite step limit are already known [27] and have been used to compute the moments of the displacement for more complex cases than are considered here [28, 29].

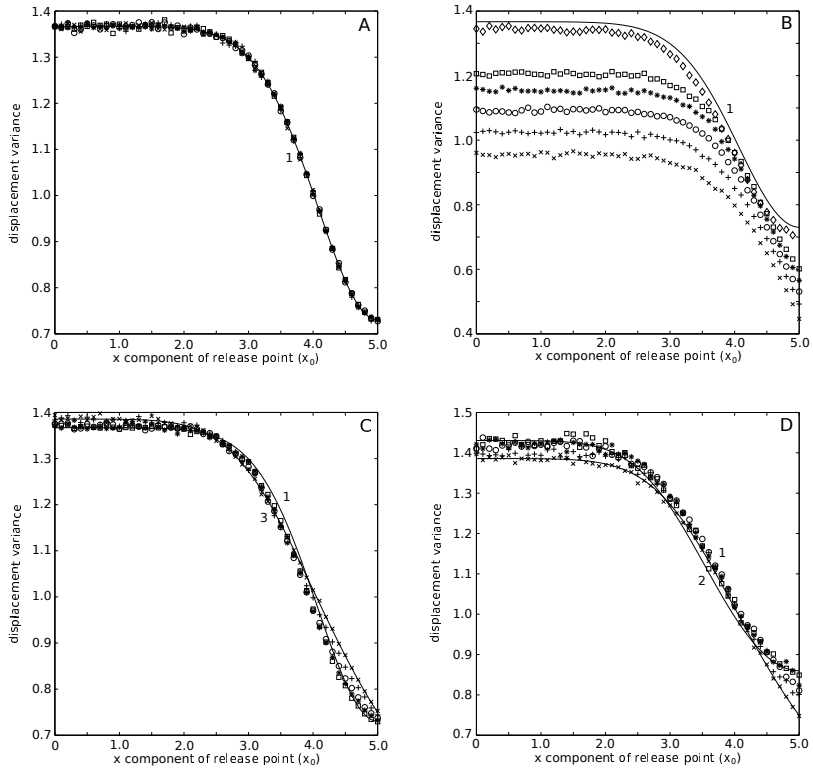

Figure 10: Cross-sections at $y_0 = 4.9$ of the variance profiles in the finite domain for impenetrable (A-C) or absorbing (D) boundaries. Solid curves were obtained analytically from decomposition into the 1d limiting cases; numbering is consistent with Fig. 4 for A-C and Fig. 5 for D. The dashed reference line shows the variance that would be obtained in unbounded space. The remaining curves (symbols) were obtained numerically using the following Δt values: 1 - $\times$, 0.5 - $+$, 0.25 - $\circ$, 0.125 - $*$, 0.0625 - $\square$, 0.001 - $\diamond$, for a reflective (A), stop-go (B), no-go (C), or absorbing (D) boundary.

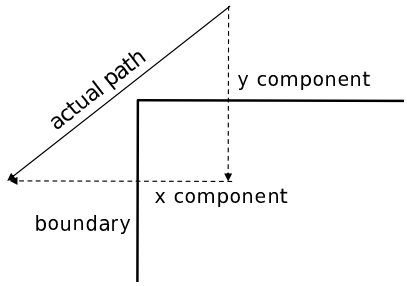

Figure 11: Sketch of path near a concave corner. Note that while the actual path never crosses the boundary the y-component does. Thus the effects of the boundary cannot be applied independently to x and y components.

characteristics. Firstly they are symmetric in the x and y axes and as such we only plot the upper right quadrant of F. Secondly, the variance returns to two, the value obtained in unbounded space, in the centre of the domain, $[-2, 2] \times [-2, 2]$. Finally, the variance is reduced along the boundaries of the domain, i.e. $y = 5$, and attains its minimum in the (convex) corners of the domain i.e. at $(5, 5)$. We note that, as we expected, in the centres of the outer boundaries, i.e. $[0, 1.5] \times [0, 5]$, the variances obtained are indistinguishable from those obtained on the half plane, see above. The similarities between profiles, and indeed the differences between them, follow naturally from the similarities and differences between the one dimensional profiles.

Variance profiles for intermediate values of Δt have similar general properties to those above, becoming more similar to the infinite step limits, i.e. Fig. 9A,D, as Δt decreases. Instead of plotting full profiles for these transitional cases, we plot a cross-section of the variance profiles (fixing $y_0 = 4.9$) for each boundary type, see Fig. 10A-D. For the reflective boundary, Fig. 10A, the limiting cases are the same and there is no transition between them. For the no-go and absorbing boundaries, Fig. 10C-D respectively, we observe that the limiting profiles shift relative to each other. For example, the variances are not equal for $x_0 \in [0, 1.5]$ where the boundary at $x = 5$ has minimal effect; thus this is clearly an effect of the other boundary at $y = 5$. In the intermediate region, $x_0 \in [2.5, 4.5]$, where this shift brings the limiting cases closer together, the transition for the absorbing boundary is not monotone, a clear difference from the behaviour observed in the semi-finite cases. Finally note that the transition for the stop-go boundary, Fig. 10, is relatively slow; even for $\Delta t = 0.001$ the variance profile has not yet reached infinite step limit.

Having investigated the time scaling behaviour within the corner of a convex domain we now move on to consider how it changes near the corners of a concave domain.

4.4. Individuals in an infinite domain with internal boundary

In the previous section we showed that individuals in a finite domain behave as if on a half plane if close to only one boundary. In the region close to two boundaries, inside a convex corner, the boundaries have a more extreme effect on behaviour but these effects remain qualitatively similar to those obtained on H. In this section we consider how the corners of a concave, rather than convex, domain influence individual behaviour. Note that, in this case, the domain is not rectangular, so the decomposition described in Section 4.1 does not apply. In addition, it can readily be shown that the x and y components, at least of discrete random walks, are not independent for any of the boundary conditions considered, see sketch in Fig. 11. This significantly complicates any analytical calculation of the mean and variance of random walks subject to these boundary conditions. As such we make use of simulated random walks, in this case in the domain $I_1 = \mathbb{R}^2/[-1,1] \times [-1,1]$, and consider a subset of release points, $[0,5] \times [0,5] \cup I_1$. (Note that while we limit the number of release points, the only constraint on movement is imposed by the internal boundary.) Variance profiles obtained for two values of Δt, 1 and 0.0625, are plotted in Fig. 12.

In this domain, unlike all others considered, the mean (not shown) and variance (Fig. 12A-B) profiles for the reflective boundary are not time scale invariant. In the one step limit the variance is significantly less that 2, the value obtained in unbounded space, along the entirety of the boundary edge, while for $\Delta t = 0.0625$ it is only reduced significantly in the centre of the boundary. Note that even here the reduction is less than is observed in the one step limit. Furthermore, in the one step limit, the variance profile appears to be split by narrow regions along the diagonals $x = y$ and $x = -y$ where the variance is approximately 2 irrespective of distance from the boundary. Note that these regions are relatively close to the (concave) corners of the boundary. For smaller values of Δt the variance profile becomes more homogeneous in this region.

The variance profiles for the stop-go and no-go boundaries, Fig. 12C-D and E-F respectively, follow the patterns that we have observed previously. In the one step limit, the stop-go boundary induces a bigger decrease in the variance than the reflective boundary and the effect of the boundary decreases similarly as the distance between the release point and the boundary increases. The effect of the no-go boundary is similar in size to that of the reflective boundary close to the boundary, but it initially decreases more quickly. For these boundary conditions there is no inhomogeneity along the diagonals of the domain. For $\Delta t = 0.0625$ the profiles for these boundaries are similar, although not identical, to that for the reflective boundary at the same Δt. The variances are generally lower for the stop-go boundary and higher for the no-go boundary.

As we would expect the variance profile for absorbing boundary, Fig. 12G, is indistinguishable from that for the no-go boundary in the one step limit. For $\Delta t = 0.0625$, the profile, Fig. 12H, is relatively homogeneous showing a gradual increase in the variance from about 1.8 units near the boundary to 2 units far from the boundary. There are small regions of lower variance, ≈ 1.7 units,

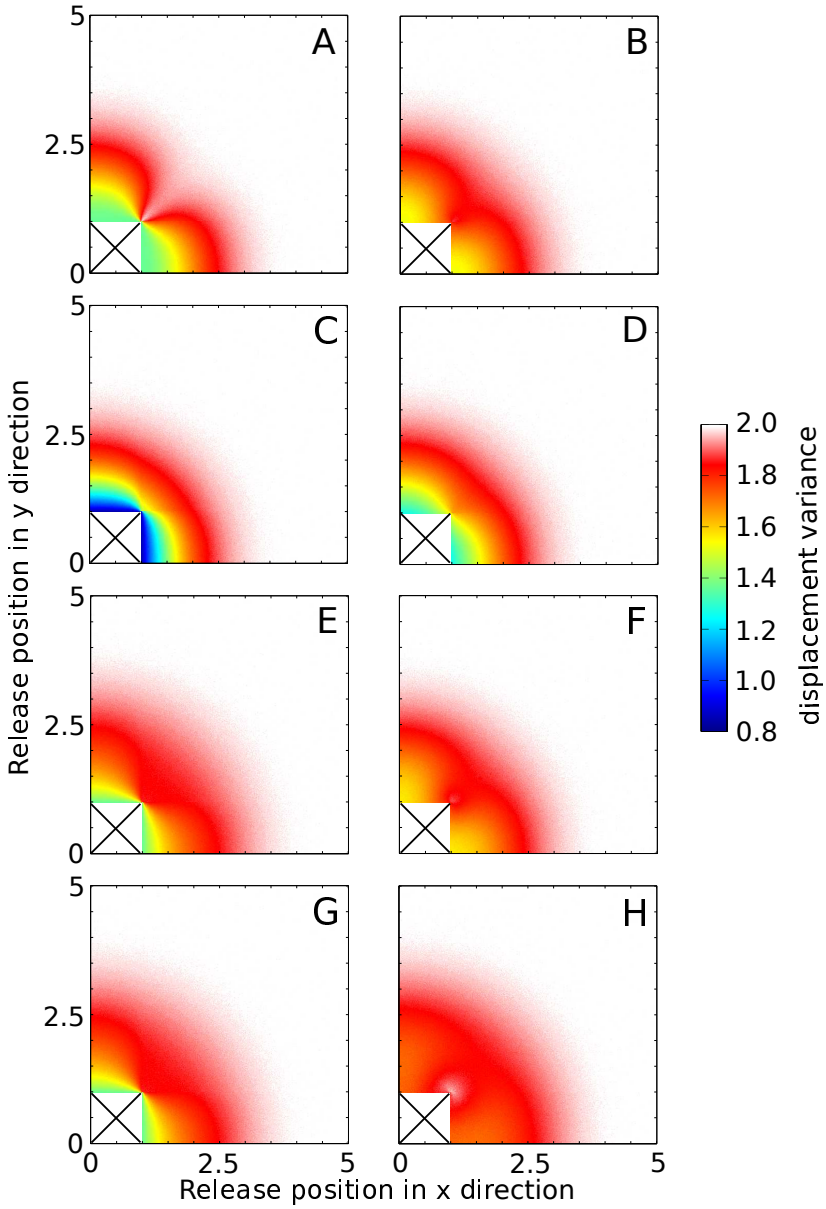

Figure 12: Variance profiles for reflective (A-B), stop-go (C-D), no-go (E-F), and absorbing (G-H) boundaries in a subset of the upper right quadrant of I_1. Profiles were calculated numerically for Δt values of 1 (left) and 0.0625 (right). The region in the lower left corner of each plot, containing a black cross, is within the internal boundary. (Color online.)

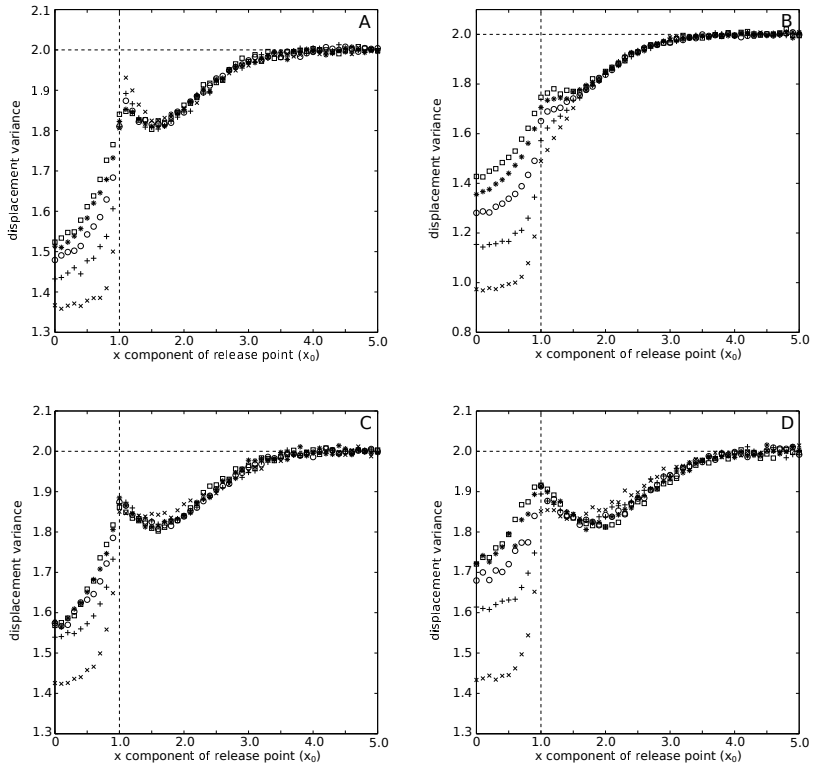

Figure 13: Cross-sections at $y_0 = 1.1$ of the variance profiles in I_1 for impenetrable (A-C) or absorbing (D) boundaries. The horizontal dashed line shows the variance that would be obtained in unbounded space. The vertical dashed line indicates the position of a corner of the internal boundary. The remaining curves (symbols) were obtained numerically using the following Δt values: 1 - $\times$, 0.5 - $+$, 0.25 - $\circ$, 0.125 - $*$, 0.0625 - $\square$, for a reflective (A), stop-go (B), no-go (C), or absorbing (D) boundary.

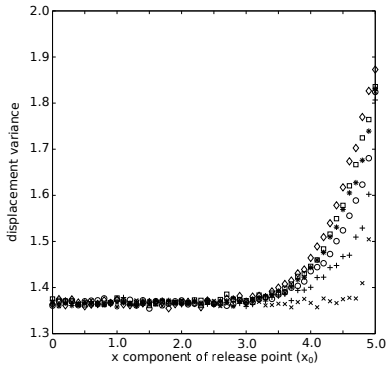

Figure 14: Cross-section at $y_0 = 5.1$ of the variance profile for a reflective boundary in the domain $I_5 = \mathbb{R}^2/[-5,5] \times [-5,5]$. The curves (symbols) were obtained numerically using the following Δt values: 1 - $\times$, 0.5 - $+$, 0.25 - $\circ$, 0.125 - $*$, 0.0625 - $\square$, 0.001 - $\diamond$.

around the x and y axes, extending from the centres of the boundaries, and a small region of higher variance, ≈ 1.9 units, near the (concave) corners of the boundary.

As in the previous section we examine the intermediate values of Δt in more detail by taking cross-sections through the variance profiles, in this case at $y_0 = 1.1$, plotted in Fig. 13A-D. In each case we see that the variance increases along the boundary $y = 1$, i.e. for $x_0 \in [0,1]$, drops briefly just beyond the corner with the boundary $x = 1$, i.e. for $x_0 < 2$, before increasing again for release points further from the boundary. There is no particularly evident loss of monotonicity in the transition processes although we should note that, for the no-go boundary, the variances obtained near $y = 1$ for $\Delta t = 0.0625$ are smaller than those obtained for the reflective boundary. Hence, assuming that the no-go variance profile will converge to that for the reflective boundary (as it does in every other case) the complete process will necessarily be non-monotonic.

Note that, for $x > 1.5$, the cross-section of the variance profile for the reflective boundary is effectively time scale invariant. The biggest differences in variance between time scales appear to occur just before the (concave) corner at $(1,1)$ is reached. We would expect that, for a sufficiently large internal boundary, the variance profile would return to that obtained in the semi-finite domain and thus that time scale invariance would be restored. To investigate how far this effect of the concave corner can extend we simulated random walks in a domain with a larger internal boundary, $I_5 = \mathbb{R}^2/[-5,5] \times [-5,5]$. A cross-section, for $y_0 = 5.1$, of the variance profiles in this domain is plotted in Fig. 14. In the single step limit the effect of the concave corner at $(5,5)$ is observed only relatively close to it ($x_0 > 4.5$). As Δt decreases this effect spreads back along the boundary eventually effecting $x_0 > 3$ for $\Delta t = 0.001$. For smaller x_0 time scale invariance is restored in all cases.

This interesting result concludes our study of two dimensional domains. In the following section we discuss the wider context of these results.

5. Discussion and conclusions

When modelling ecological movement using random walks it is generally beneficial to choose a random walk that produces behaviour which can be made independent of the choice of time scale. The framework required to do this in unbounded space is well established. However, the effects of boundaries on time scaling behaviour is relatively unexplored. In this work we have investigated how different boundary conditions affect time scale invariance of the mean squared displacement of Brownian random walks. Our key results are as follows:

1. Loss of time scale invariance is typically associated with non-conservative boundary conditions, that is, those boundary conditions which cause some part of the random walk to be discarded.
2. It is possible to determine whether time scale invariance will be lost by considering two relatively simple limiting cases in a one dimensional (sub)-system. Exact solutions for these limiting cases can be determined using analysis of the pdf generating the random walk and the diffusion equation.
3. These one dimensional results can be extended directly to two dimensional systems where the components of the random walk remain independent when subject to a boundary encounter and the domain itself is rectangular. In such cases the drift and diffusion rates are obtained by summing those obtained in a one dimensional system. Where these conditions are not met a formal two dimensional analysis is required and the time scale invariance of even the conservative, reflective, boundary condition can be lost.
4. The drift and diffusion rates close to an absorbing boundary increase as the random walk used becomes finer. As discussed in Section 3.3 this phenomenon results from an increased chance to leave the domain for smoother random walks.

In the majority of cases where time-scale invariance is lost the drift and diffusion rates for intermediate values of Δt shift monotonically from one limiting case to the other. Where this is the case it may be possible to approximate the intermediate profiles by taking a suitably weighted average of the limiting cases. Typically this transition is not monotone when the limiting cases are relatively close together for a large range of release points and intersect somewhere in this range. In such cases, the mean and variance profiles pass through the infinite step limit as Δt decreases before converging back to it, cf Figs. 4E-F and 10C-D. A weighted average is clearly not appropriate in such cases, but given that the process remains relatively simple some mathematical description of the process should be possible. Investigation of these possibilities provides one potential avenue for further work in this area.

In a broader context, we should ask whether the observed loss of time scale invariance has an impact on a longer time scale. Models of individual movement

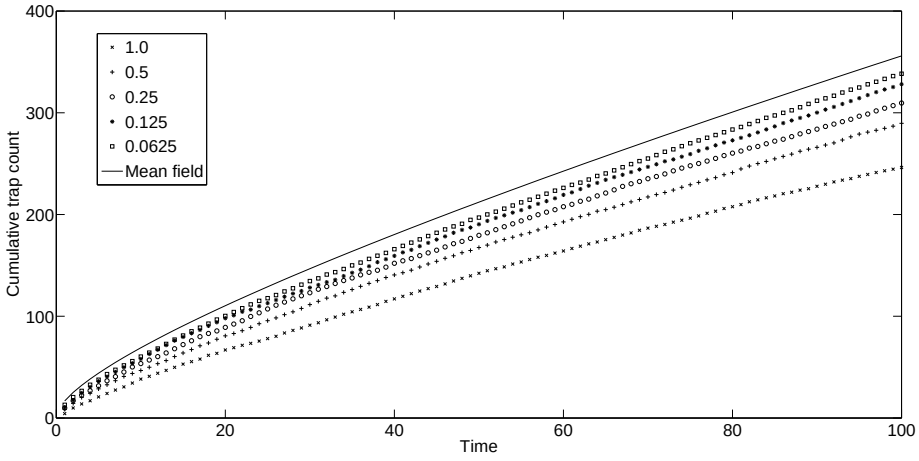

Figure 15: Trap count trajectories plotted against time. Solid curve corresponds to the solution obtained from the diffusion equation, $D = 1.0$. Remaining curves produced from simulated random walks (Δt in the inset key) with the same effective speed.

will rarely only consider a single unit of time, and consequently relatively long random walks will typically be used. One might assume that this allows all such models to be treated as if in the diffusion limit, thus circumventing this problem.

One application of the random walk framework is in the analysis of pest insect trap counts [14, 30]. The cummulative number of individuals trapped from a population performing a Brownian random walk can be simulated numerically or predicted from the diffusion equation. Trajectories of these cummulative trap counts obtained for the range of Δt values used throughout this work ($\Delta t = \{1.0, 0.5, 0.25, 0.125, 0.0625\}$) differ from that obtained from the diffusion solution and each other, Fig. 15, despite having the same dispersal rate D. All of these random walks contain at least 100 steps so it is clear that the effects of loss of time scale invariance do not disappear for long random walks.

In conjunction with point 4) above, this long term effect of time scale on interactions with an absorbing boundary is particularly important in the context of climate change and habitat fragmentation. The effect of dispersal out of shrinking habitats on a population's dynamics have been a topic of much recent research, see for example [31, 32]. Models of the problem make use of dispersal kernels which vary with spatial position. When designing these kernels, or parameterising them from data, the interaction between the time scale of the individual's movement and the effect of the boundary must be taken into account.

Mean field approximations, such as the diffusion equation, are very useful tools for the study of dispersing populations as they provide a direct link between model dynamics and parameters, see for example [3]. However, where time scale invariance is lost, they only exactly describe a limiting case of the movement

behaviour, i.e. where $\Delta t \to 0$. Where this condition does not apply, say for a movement model with a correlation between subsequent steps (such as the Correlated Random Walk [33]) which becomes Brownian only for relatively large Δt, a correction must be applied to the solution of the mean field equation. This work provides the basis on which such a correction technique can be developed.

Empirical studies of animal movement often make use of random walk models. Where the domain of movement is confined the boundary effects outlined in this paper will, naturally, influence any estimates of the drift and diffusion rates of individuals. Indeed Giuggioli et al. show how these estimates may be affected by the size of a finite domain with impenetrable boundaries for smooth random walks [28]. Of course, as this work has shown, the size of the domain is not the only factor which influences such estimates. Where the movement of individuals is most naturally approximated by a discrete random walk, or if, as above, a correlated random walk should be used, the time scale of the walk becomes an important factor. In such cases it may be possible to estimate the natural time scale of the animal movement by comparing estimates of drift and diffusion rates in confined and unconfined domains.

Acknowledgments

This work was supported by The Leverhulme Trust through grant F/00-568/X.

References

[1] Murray, J.D. 1989, Mathematical biology, London: Springer.

[2] Turchin, P. 1998, Quantitative analysis of animal movement, Sunderland: Sinauer.

[3] Mendez, V., Campos, D., & Bartumeus, F. 2014, Stochastic foundations in movement ecology: Anomalous diffusion, front propagation and random searches, Berlin: Springer.

[4] Sheratt, J.A., Lewis, M.A., & Fowler, A.C. 1995 Ecological chaos in the wake of invasion, *Proc. Natl. Acad. Sci.* 92:2524-2528. (DOI 10.1073/pnas.92.7.2524)

[5] Adamson, M.W., & Morozov, A.Y. 2012 Revising the role of species mobility in maintaining biodiversity in communities with cyclic competition, *Bull. Math. Biol.* 74:2004-2031. (DOI 10.1007/s11538-012-9743-z)

[6] Grimm, V., & Railsback S.F. 2005, Individual-based modelling and ecology, Princeton: Princeton University Press.

[7] Moorcroft, P.R., & Barnett, A. 2008 Mechanistic home range models and resource selection analysis: a reconciliation and unification, *Ecology* 89(4), 1112-1119. (DOI 10.1890/06-1985.1)

[8] Preisler, H.K., Ager, A.A., & Wisdom, M.J. 2013, Analyzing animal movement patterns using potential functions. *Ecosphere*, 4(3): article 32. (DOI: 10.1890/es12-00286.1)

[9] Berg, H.C. 1983, Random walks in biology, Princeton: Princeton University Press.

[10] Codling, E.A., Plank, M.J., & Benhamou, S. 2008 Random walk models in biology, *J. R. Soc. Interface* 5:813-834. (DOI 10.1098/rsif.2008.0014)

[11] Turchin, P. & Thoeny, W.T. 1993 Quantifying dispersal of southern pine beetles with mark-recapture experiments and a diffusion model, *Ecol. Appl.* 3(1):87-198. (DOI 10.2307/1941801)

[12] Viswanathan, G.M., Buldyrev, S.V., Havlin, S., Da Luz, M.G.E., Raposo, E.P., & Stanley, H.E. 1999 Optimizing the success of random searches, *Nature* 401:911-914. (DOI 10.1038/44831)

[13] Bartumeus, F., da Luz, M.G.E., Viswanathan, G.M., & Catalan, J. 2005 Animal search strategies: a quantitative random-walk analysis. *Ecology*, 86(11):3078-3087. (DOI 10.1890/04-1806)

[14] Petrovskii, S.V., Bearup, D., Ahmed, D.A., & Blackshaw, R. 2012 Estimating insect population density from trap counts, *Ecol. Complex.*, 10, 69-82. (DOI 10.1016/j.ecocom.2011.10.002)

[15] Potts, J.R., Bastille-Rousseau, G., Murray, D.L., Schaefer, J.A., & Lewis, M.A. 2014, Predicting local and non-local effects of resources on animal space use using a mechanistic step selection model, *Methods Ecol. Evol.*, 5:253-262. (DOI 10.1111/2041-210X.12150)

[16] Sornette, D. 2003, Critical phenomena in natural sciences, 2nd edn., Berlin: Springer.

[17] Hernández-Garcia, E., Pesquera, L., Rodriguez, M.A., & San Miguel, M. 1987 First-passage time statistics: Processes driven by Poisson noise, *Phys. Rev. A* 36(12), 5774-5781. (DOI 10.1103/PhysRevA.36.5774)

[18] Balescu, R. 1975, Equilibrium and nonequilibrium statistical mechanics, New York: John Wiley.

[19] Einstein, A. 1905 On the movement of small particles suspended in stationary liquids required by the molecular-kinetic theory of heat, *Ann. Phys.* 322(8), 549-560. (DOI 10.1002/andp.19053220806)

[20] Crank, J. 1975, The mathematics of diffusion, Oxford, UK: Oxford University Press.

[21] Forester, J.D., Im, H.K., & Rathouz, P.J. 2009, Accounting for animal movement in estimation of resource selection functions: sampling and data analysis, *Ecology* 90(12):3554-3565. (DOI 10.1890/08-0874.1)

[22] Grimmett, G. & Stirzaker, D. 2001, Probability and random process. Oxford, UK: Oxford University Press.

[23] Leone, F.C., Nelson, L.S., & Nottingham R.B. 1961, The folded normal distribution, *Technometrics*, 3(4):543-550. (DOI 10.2307/1266560)

[24] Aslangul, C. 1999, Diffusion of two repulsive particles in a one-dimensional lattice, *J Phys A: Math. Gen.* 32:3993-4003. (DOI 10.1023/a:1004548430438)

[25] Tikhonov, A.N. & Samarskii, A.A. 1990, Equations of mathematical physics. Dover books on physics, Vol. 39. New York, USA: Dover Publications.

[26] Chandrasekhar, S. 1943, Stochastic Problems in Physics and Astronomy, *Rev. Mod. Phys.*, 15(1):1-89. (DOI 10.1103/RevModPhys.15.1)

[27] Carslaw, H.S. & Jaeger, J.C. 1959, Conduction of heat in solids. Oxford, UK: Oxford University Press.

[28] Giuggioli, L., Abramson, G., Kenkre, V.M., Suzán, G., Marcé, E., & Yates, T.L. 2005, Diffusion and home range parameters from rodent population measurements in Panama, *B. Math. Biol.* 67(5):1135-1149. (DOI 10.1016/j.bulm.2005.01.003)

[29] Giuggioli, L., Potts, J.R., & Harris, S. 2012. Predicting oscillatory dynamics in the movement of territorial animals, *J. R. Soc. Interface*, 9(72):1529-1543. (DOI 10.1098/rsif.2011.0797)

[30] Petrovskii, S.V., Petrovskaya, N., & Bearup, D. 2014 Multiscale approach to pest insect monitoring: Random walks, pattern formation, synchronisation and networks, *Phys. Life Rev.* 11(3):467-525. (DOI 10.1016/j.plrev.2014.02.001)

[31] Van Kirk, R.W. & Lewis, M.A. 1997, Integrodifference models for persistence in fragmented habitats, *B. Math. Biol.*, 59(1):107-137. (DOI 10.1007/bf02459473)

[32] Zhou, Y. & Kot, M. 2011, Discrete-time growth-dispersal models with shifting species ranges, *Theor. Ecol.*, 4:13-25. (DOI 10.1007/s12080-010-0071-3)

[33] Kareiva, P.M. & Shigesada, N. 1983, Analyzing insect movement as a correlated random walk, *Oecologia*, 56(2-3):234238. (DOI 10.1007/bf00379695)

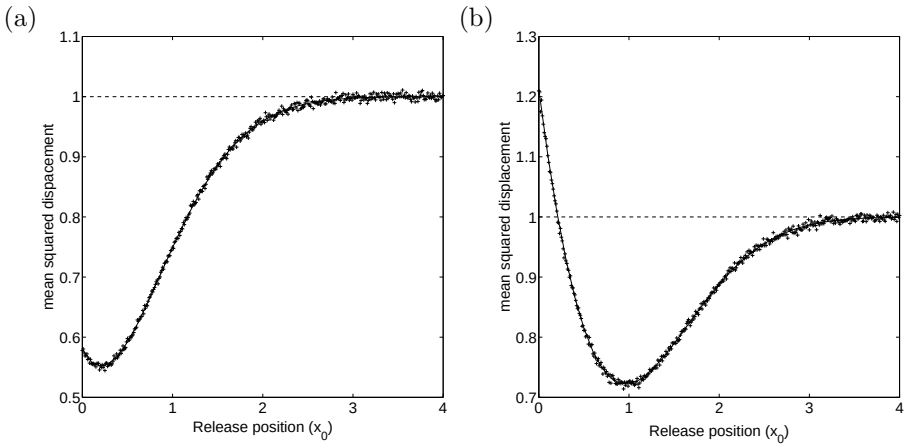

Figure A.16: Mean square displacement profiles for two step random walks. Solid curves obtained by numerical evaluation of the position pdf obtained by convolution, details in the text. The remaining curves are as described in the figures in Section 3. (a) With a stop-go boundary; (b) With an absorbing boundary.

Appendix A. Analytical derivation of pdfs for intermediate Δt in 1D

It is possible to extend the method used to obtain the profiles for one step limit, see Section 3, to other values of Δt. The position pdf for these cases can be derived by inductive convolution of the appropriate kernel, i.e.:

$$f^{(n)}(x_1; x_0, \sigma^2) = \int_0^\infty f^*(x_1; y, \cdot) f^{(n-1)}(y; x_0, \cdot) dy, \tag{A.1}$$

where f^* denotes $f^{(1)}$ and y is a dummy variable. For the Neumann boundary condition the kernel is simply the position pdf for the corresponding boundary condition, taking into account the need to rescale the standard deviation. Thus for the reflective boundary condition we take $f^* = f'_r(x_1; x_0, \sigma^2/2)$. The position pdf (considering only possible positions) for the second step is then:

$$f^{(2)}(x_1; x_0, \sigma^2) = \int_0^\infty f'_r(x_1; y, \tfrac{\sigma^2}{2}) f'_r(y; x_0, \tfrac{\sigma^2}{2}) dy. \tag{A.2}$$

In this case a closed form of the right hand side can be found as follows. We begin by substituting in the definition of f'_r, Table 1(i), and multiplying out terms to obtain:

$$f^{(2)}(x_1; x_0, \sigma^2) = \int_0^\infty f_{x_1,y} f_{y,x_0} + f_{x_1,y} f_{-y,x_0} + f_{-x_1,y} f_{y,x_0} + f_{-x_1,y} f_{-y,x_0} dy, \tag{A.3}$$

where $f_{a,b}$ denotes $f(a;b,\sigma^2/2)$. Collecting the first and fourth terms and noting that $(-x+y)^2 = (-y+x)^2$ we see that:

$$\int_0^\infty f_{x_1,y}f_{y,x_0} + f_{-x_1,y}f_{-y,x_0}dy = \int_0^\infty f_{x_1,y}f_{y,x_0} + f_{x_1,-y}f_{-y,x_0}dy, \tag{A.4}$$

$$= \int_0^\infty f_{x_1,y}f_{y,x_0}dy + \int_{-\infty}^0 f_{x_1,y}f_{y,x_0}dy, \tag{A.5}$$

$$= \int_{-\infty}^\infty f_{x_1,y}f_{y,x_0}dy. \tag{A.6}$$

But it is known that the convolution of two Gaussian functions (on $\mathbb{R}$) produces another Gaussian function with variance equal to the sum of the variances of the original function, thus:

$$\int_0^\infty f_{x_1,y}f_{y,x_0} + f_{-x_1,y}f_{-y,x_0}dy = f(x_1;x_0,2\tfrac{\sigma^2}{2}) = f(x_1;x_0,\sigma^2). \tag{A.7}$$

By a similar sequence of manipulations we can also obtain:

$$\int_0^\infty f_{x_1,y}f_{-y,x_0} + f_{-x_1,y}f_{y,x_0}dy = f(-x_1;x_0,2\tfrac{\sigma^2}{2}) = f(-x_1;x_0,\sigma^2). \tag{A.8}$$

So Eq. (A.2) becomes:

$$f^{(2)}(x_1;x_0,\sigma^2) = f(x_1;x_0,\sigma^2) + f(-x_1;x_0,\sigma^2), \tag{A.9}$$

which is exactly $f'_r(x_1;x_0;\sigma^2)$. This proves analytically that the reflective implementation of the impenetrable boundary condition preserves time scale invariance.

For the stop-go boundary condition it is not typically possible to obtain a convenient closed form of the convolution. Nonetheless it is possible to evaluate it numerically, see Fig. A.16(a). The no-go and absorbing boundaries are identical in the one step limit. However for random walks with more steps they behave differently. This arises because in for the no-go boundary individuals always remain within the domain, while for the absorbing boundary individuals are removed at each time step and an average is taken over the individuals remaining. Thus the correction factor converting the function obtained into a proper pdf is applied only after the final time step. Taking $f^* = f'_n = f'_a$ results in the appropriate pdf for the no-go boundary. For the absorbing boundary we take:

$$f^*(x_1;x_0,\tfrac{\sigma^2}{n}) = \begin{cases} f(x_1;x_0,\frac{\sigma^2}{n}) & x_1 > 0 \\ 0 & x_1 \leq 0 \end{cases}, \tag{A.10}$$

and apply the correction factor, $\alpha(x_0) = 1/\int_0^\infty f^{(n)}(x_1;x_0,\sigma^2)$, to $f^{(n)}$. Again it is typically impossible to obtain closed forms of the resulting position pdf but numerical solutions can be obtained, see Fig. A.16(b) for an example using the absorbing boundary condition.